Oceanic emissions unlikely to account for the missing source of atmospheric carbonyl sulfide

Sinikka T. Lennartz[1], Christa A. Marandino[1], Marc von Hobe[2], Pau Cortes[3], Birgit Quack[1], Rafel Simo[3], Dennis Booge[1], Andrea Pozzer[4], Tobias Steinhoff[1], Damian L. Arevalo-Martinez[1], Corinna Kloss[2], Astrid Bracher[5,6], Rüdiger Röttgers[7], Elliott Atlas[8], and Kirstin Krüger[9]

[1]GEOMAR Helmholtz-Centre for Ocean Research Kiel, Düsternbrooker Weg 20, 24105 Kiel, Germany
[2]Forschungszentrum Jülich GmbH, Institute of Energy and Climate Research (IEK-7),Wilhelm-Johnen-Strasse, 52425 Jülich, Germany
[3]Institut de Ciencies del Mar, CSIC, Pg. Maritim de la Barceloneta, 37-49, 08003 Barcelona, Catalonia, Spain
[4]Max-Planck-Institute for Chemistry, Hahn-Meitner-Weg 1, 55128 Mainz, Germany
[5]Alfred-Wegener-Institute Helmholtz Center for Polar and Marine Research, Bussestrasse 24, 27570 Bremerhaven, Germany
[6]Institute of Environmental Physics, University of Bremen, 28334 Bremen, Germany
[7]Helmholtz-Zentrum Geesthacht, 21502 Geesthacht, Germany
[8]Rosenstiel School of Marine and Atmospheric Science, Miami, FL 33149 Florida, USA
[9]University of Oslo, Department of Geosciences, 0315 Oslo, Norway

Correspondence to: S. T. Lennartz (slennartz@geomar.de)

Abstract. The climate active trace-gas carbonyl sulfide (OCS) is the most abundant sulfur gas in the atmosphere. A missing source in its atmospheric budget is currently suggested, resulting from an upward revision of the vegetation sink in top-down approaches. Oceanic emissions have been proposed to close the resulting gap in the atmospheric budget. We present a bottom-up approach including new observations of OCS in surface waters of the tropical Atlantic, Pacific and Indian oceans to show that direct OCS emissions are insufficient to account for the missing source. Extrapolation of our observations using a biogeochemical box model suggests oceanic net uptake instead of emission for the entire tropical ocean area and, further, a global ocean source strength well below that suggested by top-down estimates. This bottom-up estimate of oceanic emissions has implications for using OCS as a proxy for terrestrial CO_2 uptake, which is currently hampered by the inadequate quantification of atmospheric OCS sources and sinks.

1 Introduction

Carbonyl sulfide (OCS) is the most abundant reduced sulfur compound in the atmosphere. It enters the atmosphere either by direct emissions, e.g. from oceans, wetlands, anoxic soils or anthropogenic emissions, or indirectly via oxidation of the short-lived precursor gases dimethylsulfide (DMS) and carbon disulfide (CS_2) (Chin and Davis, 1993; Watts, 2000; Kettle, 2002). Both precursor gases are naturally produced in the oceans, and CS_2 has an additional anthropogenic source (Kettle, 2002; Stefels et al., 2007; Campbell et al., 2015). Combining direct and indirect marine emissions, the ocean is considered as the dominant source of atmospheric OCS (Chin and Davis, 1993; Watts, 2000; Kettle, 2002). The most important sink of atmospheric OCS is uptake by terrestrial vegetation (Campbell et al., 2008) and oxic soils, while chemical loss by photolysis

and reaction with the hydroxyl radical (OH) in the atmosphere are minor loss processes (Chin and Davis, 1993; Watts, 2000; Kettle, 2002). While tropospheric volume mixing ratios show a distinct annual cycle (Montzka et al., 2007), the interannual to decadal variation is low (Montzka et al., 2007; Kremser et al., 2015).

Accurate accounts of sources and sinks of atmospheric OCS are crucial for two reasons.

5   – First, OCS is climate-relevant because it influences the radiative budget of the Earth as a greenhouse gas and by contributing significant amounts of sulfur to the stratospheric aerosol layer (Brühl et al., 2012; Notholt et al., 2003; Turco et al., 1980) that exerts a cooling effect (Crutzen, 1976; Kremser et al., 2016). The two opposite effects are currently in balance (Brühl et al., 2012), but future changes in atmospheric circulation, as well as the magnitude and distribution of OCS sources and sinks, could change that. Hence, a better understanding of the tropospheric budget is needed to predict

10   the effect of OCS in future climate scenarios (Kremser et al., 2016).

   – Second, OCS has recently been suggested as a promising tool to constrain terrestrial CO_2 uptake, i.e. gross primary production (GPP), as it is taken up by plants in a similar way as CO_2 (Asaf et al., 2013). GPP, a major global CO_2 flux, can only be inferred from indirect methods, because the uptake of CO_2 occurs along with a concurrent release by respiration. Unlike CO_2, OCS is irreversibly degraded within the leaf. GPP can thus be estimated based on the uptake

15   ratio of OCS and CO_2, from the leaf to regional scale (Asaf et al., 2013) or even global scale (Beer et al., 2010), under the condition that other sources are negligible or well quantified. The magnitude of terrestrial biogeochemical feedbacks on climate has been suggested to be similar to that of physical feedbacks (Arneth et al., 2010). In order to reduce existing uncertainties, it is thus crucial to better constrain single processes in the carbon cycle, especially GPP.

Nonetheless, current figures for tropospheric OCS sources and sinks carry large uncertainties (Kremser et al., 2016). Recent

20 sources and sinks inferred from top-down approaches (Suntharalingam et al., 2008; Berry et al., 2013; Kuai et al., 2015; Glatthor et al., 2015) do not match observation-based bottom-up approaches (Kettle, 2002). While the budget was previously considered closed (Kettle, 2002), a recent upward revision of the vegetation sink (Suntharalingam et al., 2008; Berry et al., 2013) led to a gap, i.e. a missing source, in the atmospheric budget of 230-800 Gg S per year (Suntharalingam et al., 2008; Berry et al., 2013; Kuai et al., 2015; Glatthor et al., 2015) (Tab. 1), with the most recent estimates at the higher end of the

25 range. This revision of vegetation uptake was needed to better reproduce observed seasonality of OCS mixing ratios in several atmospheric models (Berry et al., 2013; Kuai et al., 2015; Glatthor et al., 2015). Based on a top-down approach using satellite observations and inverse modelling, the missing source of OCS was suggested to originate from the tropical ocean (Kuai et al., 2015; Glatthor et al., 2015). This missing source must thus be added on top of direct and indirect oceanic emissions estimated in earlier studies. This addition would imply a 200-380% increase of the *a priori* estimated oceanic source. If oceanic direct

30 and indirect emissions were to account for the total missing source, an ocean source strength of 465-1089 Gg S yr^{-1} would be required (Tab. 1).

OCS and its atmospheric precursors are naturally produced in the ocean. OCS is produced photochemically from chromophoric dissolved organic matter (CDOM) (Andreae and Ferek, 2002; Ferek and Andreae, 1984) and by a not fully understood light independent production pathway that depends on temperature and CDOM concentration (Flöck et al., 1997;

Von Hobe et al., 2001). Dissolved OCS is efficiently hydrolyzed to CO_2 and H_2S at a rate depending on pH and temperature (Elliott et al., 1989). CS_2 is produced photochemically (Xie et al., 1998) and biologically (Xie et al., 1999), and no significant loss process other than air-sea gas exchange has been identified (Xie et al., 1998). DMS is biogenically produced and consumed in the surface ocean, as well as photo-oxidized and ventilated by air-sea exchange (Stefels et al., 2007).

5   Available bottom-up estimates of the global oceanic OCS fluxes from shipboard observations range from -16 Gg S yr^{-1} to 320 Gg S yr^{-1} (Tab. 2). However, the highest estimates were biased, because mainly summertime and daytime observations of water concentrations were considered. With the discovery of the seasonal oceanic sink of OCS during wintertime (Ulshöfer et al., 1995) and a pronounced diel cycle (Ferek and Andreae, 1984), direct oceanic emissions were corrected downwards.

Only recently, OCS emissions have been estimated with the biogeochemical ocean model NEMO-PISCES (Launois et al.,
10   2015a) at a magnitude of 813 Gg S yr^{-1}, sufficient to account for the missing source. This oceanic emission inventory has been used in a first attempt to constrain GPP based on OCS on a global scale (Launois et al., 2015b). However, the oceanic OCS photoproduction in the ocean model included a parameterization for OCS photoproduction derived from an experiment in the North Sea (Uher and Andreae, 1997b), which might not be representative for the global ocean.

Here, we quantify OCS emissions from these regions based on direct observations to resolve this discrepancy and to conclu-
15   sively answer the question of whether the missing OCS source identified in the atmospheric top-down approaches can really be ascribed to the direct OCS emission from tropical oceans. Fluxes were directly inferred from continuous OCS measurements in the tropical Pacific and Indian Oceans, covering a range of regimes with respect to CDOM content, ultraviolet radiation (UV) and sea surface temperature (SST). A time resolution on the order of minutes allowed for an accurate integration over full diel cycles. The new data are complemented by measurements obtained at coarser resolution across the Atlantic Ocean. The
20   observations were further used to improve a state of the art box model of the production and consumption processes, which was then employed to estimate oceanic OCS emissions on the global scale.

2 Methods

2.1 Measurement set-up for trace gases

OCS was measured during two cruises on board the R/V SONNE I (OASIS) and SONNE II (ASTRA-OMZ) with a continuous
25   underway system (Arévalo-Martínez et al., 2013) at a measurement frequency of 1 Hz. The system consisted of a Weiss-type equilibrator, through which seawater is pumped from approximately 5 m below the surface with a flow of 3-4 L min^{-1}. The air from the equilibrator headspace was Nafion dried and continuously pumped into an OCS-analyzer (Model DL-T-100, Los Gatos Research) that uses off axis - integrated cavity output spectroycopy (OA-ICOS) technique. The instrument used on board is a prototype of a commercial instrument (www.lgrinc.com/documents/OCS_ Analyzer_ Datasheet.pdf), developed by
30   Los Gatos Research (LGR) in collaboration with Forschungszentrum Jülich GmbH (Schrade, 2011). Data were averaged over 2 minutes, achieving a precision of 15 ppt. OCS mixing ratios in the MBL were determined by pumping outside air ca. 50 m from the ship's deck to the OCS analyzer (KNF Neuberger pump). A measurement cycle consisted of 50 min water sampling and 10 min air sampling, where the first 3 minutes after switching until stabilization of the signal were discarded.

Before and after the cruise the analyzer was calibrated over a range of concentrations using permeation devices. Both calibrations were consistent. However, the output of the internal spectral retrieval differed significantly from post processing of the recorded spectra, which matched the known concentrations (this offset is not present in the commercial instruments). The calibration data were thus used to derive a correction function. After correction all data stayed within 5% of the standards. The

5   calibration scale of the permeation devices was 5% below the NOAA scale. As the OCS analyzer measured CO_2 simultaneously, and CO_2 standards were available during the cruise, drift of the instrument was tested by measuring CO_2 standard gases before and after the cruise and found to be less than 1% of the signal. Special care was taken to avoid contamination and all materials used have been tested for contamination before use.

During OASIS, the mirrors inside the cavity of the OCS analyzer were not completely clean, which led to a reduced signal.

10   To correct the data, an attenuation factor was determined from simultaneous CO_2 measurements, because no OCS standard was available onboard, and OASIS data was corrected accordingly.

An independent quality check of the data was performed by comparing volume mixing ratios of the MBL from the OCS analyzer with samples from air canisters sampled during both cruises and measured independently (Schauffler et al., 1998; de Gouw et al., 2009). The calibrated (and attenuation corrected for OASIS) OA-ICOS data were on average 5% lower than

15   the air canister samples, which reflects the 5% difference between the calibration at Forschungszentrum Jülich and the NOAA scale.

During ASTRA-OMZ, CS_2 was directly measured on board within 1 hour of collection using a purge and trap system attached to a gas chromatograph and mass spectrometer (GC/MS; Agilent 7890A/Agilent 5975C; inert XL MSD with triple axis detector) running in single ion mode. The discrete surface seawater samples (50 mL) were taken each hour to every three

20   hours from the same pump system as for continuous OCS measurements. CS_2 was stripped by purging with helium (70 mL min^{-1}) for 15 minutes. The gas stream was dried using a Nafion membrane dryer (Perma Pure) and CS_2 was preconcentrated in a trap cooled with liquid nitrogen. After heating the trap with hot water, CS_2 was injected into the GC/MS. Retention time for CS_2 (m/z 76, 78) was 4.9 minutes. The analyzed data was calibrated each day using gravimetrically prepared liquid CS_2 standards in ethylene glycol. While purging, 500 μL gaseous deuterated DMS (d3-DMS) and isoprene (d5-isoprene) were

25   added to each sample as an internal standard to account for possible sensitivity drift between calibrations.

During the TransPEGASO cruise on board R/V Hesperides, surface ocean OCS and CS_2 were measured in discrete seawater samples by purge and trap and gas chromatography with mass spectrometry detection (GC-MSD). Samples were collected every day at 9:00 and 15:00 h local time in glass bottles without headspace and analyzed within 1 hour. Aliquots of 25 mL were withdrawn with a glass syringe and filtered through GF/F while injected into the purge and trap system (Stratum, Teledyne

30   Tekmar). The water was heated to 30°C and volatiles were stripped by bubbling with 40 mL min-1 of ultrapure helium for 12 minutes and trapped in a U-shaped VOCARB 9 trap at room temperature. After flash thermal desorption, volatiles were injected into an Agilent 5975T LTM GC-MSD equipped with an Agilent LTM DB-VRX column (20 m x 0.18 mm OD x 1μm) maintained at 30°C. Retention times for OCS (m/z 60) and CS_2 (m/z 76) were 1.3 and 2.7 min, respectively. Peak quantification was achieved with respect to gaseous (OCS in N_2) and liquid (CS_2 in methanol and water) standards that were analyzed in the

same way. Samples were run in duplicates. Detection limits were 1.8 pM (OCS) and 1.4 pM (CS_2), and precision was typically around 5%.

2.2 Calculation of air-sea exchange

Fluxes F of all gases were calculated with Eq. 1:

$$5 \quad F = k_w \cdot \Delta C \tag{1}$$

where k_w is the gas transfer velocity in water (i.e. physical constraints on exchange) and ΔC the air-sea concentration gradient (i.e. the chemical constraint on exchange). The air-side transfer velocity (Liss and Slater, 1974) for OCS was calculated to be seven orders of magnitude smaller and was therefore neglected. The concentration gradient was determined using the temperature dependent Henry constantv (De Bruyn et al., 1995) and the measurements in the surface water and MBL for

10 OASIS and ASTRA-OMZ. During TransPEGASO, no atmospheric volume mixing ratio was measured, and a value of 500 ppt was assumed (Montzka et al., 2007). The transfer velocity k_w was determined using a quadratic parameterization based on wind speed (Nightingale et al., 2000) which was directly measured onboard (10 minute averages). Furthermore k_w was corrected for OCS and CS_2 by scaling it with the Schmidt number calculated from the molar volume of the gases (Hayduk and Laudie, 1974). It should be noted that the choice of the parameterization for k_w has an non-negligible influence on the

15 global emission estimate. Linear, quadratic and cubic parameterizations of k_w are available, with differences increasing at high wind speeds in the order of a factor of 2 (Lennartz et al., 2015; Wanninkhof et al., 2009). Evidence suggests that the air-sea exchange of insoluble gases such as CO_2, OCS and CS_2, follows a cubic relationship to wind speed because of bubble-mediated gas transfer (McGillis et al., 2001; Asher and Wanninkhof, 1998). However, this difference between soluble and non-soluble gases is not always consistent (Miller et al., 2009), and too little data is available for a reliable parameterization

20 at high wind speeds above 12 m s^{-1}, where the cubic and the quadratic parameterizations diverge the most. For reasons of consistency, e.g. for the fitted photoproduction p from previous studies, and the fact that most of the previous emission estimates were computed using a quadratic k_w parameterization, we chose the same quadratic parameterization representing the mean range of observations (Nightingale et al., 2000). For a sensitivity test, we computed the global oceanic emission with a cubic relationship (McGillis et al., 2001), which results in an additional 40 Gg S per year as direct OCS emissions, leaving

25 the missing source still explained. However, better constraints on the transfer velocity of insoluble gases would decrease the uncertainty of global oceanic emissions of marine trace gases.

2.3 Box model of OCS concentration in the surface ocean

The box model (von Hobe et al., 2003) included parameterizations for hydrolysis (Elliott et al., 1989), air-sea exchange (Nightingale et al., 2000), light-independent production (Von Hobe et al., 2001) and photochemical production (von Hobe

30 et al., 2003; Weiss et al., 1995a). Photoproduction was integrated over the mixed layer depth (MLD), assuming a constant concentration of OCS and CDOM throughout the mixed layer, with the photoproduction rate constant p [mol J^{-1}], a$_{350}$ [m^{-1}]

and the UV [W m^{-2}] (Sikorski and Zika, 1993) (Eq. 2).

$$\frac{dC_{OCS}}{dt} = \int\limits_{-MLD}^{0} p a_{350} UV dz \tag{2}$$

MLD was obtained from CTD profiles and interpolated between these locations (S-Fig 1,2). The photochemically active radiation that reaches the ocean surface was approximated by Eq. 3 (Najjar et al., 1995):

$$UV = 2.85 \cdot 10^{-1} \cdot I \cdot cos^2\theta \tag{3}$$

with global radiation I [W m^{-2}] and the zenith angle cos θ. The attenuated UV light intensity directly below the surface (Sikorski and Zika, 1993) down to the respective depth of the mixed layer was calculated in 1 m steps, taking into account attenuation by CDOM and pure seawater. As a simplification in this global approach, the box model did not resolve the whole wavelength spectrum, but rather used a$_{350}$ and applied a photoproduction rate constant that takes into account the integrated spectrum. A similar approach had been tested and compared to a wavelength spectrum resolving version by von Hobe et al. (2003).

The photoproduction constant in the case study simulations was fitted individually for periods of daylight >100 W m^{-2} (Fig. 2, blue lines). The rate constant p was fitted with a Levenberg-Marquart optimization routine in MatLab version 2015a (8.5.0), by minimizing residuals between simulated and hourly averaged measurements. Different starting values were tested to reduce the risk of the fitted p being a local minimum. Together with photoproduction rate constants obtained by a similar optimization procedure by von Hobe et al. (2003) (Tab. 2 therein, termed MLB STC), a relationship of the photoproduction constant p dependent on a$_{350}$ was established (Fig. 3). The resulting linear relationship thus includes values from the Altantic, Pacific and Indian Ocean, making it a good approximation for a globally valid dependence. For the global box model, p was calculated in every time step based on this relationship (Eq. 4):

$$p = 3591.3 \cdot a_{350} + 329.4 \tag{4}$$

OCS is also produced by a light-independent production term, which was parameterized depending on SST [K] and a$_{350}$ (Von Hobe et al., 2001) (Eq. 5).

$$\frac{dC_{OCS}}{dt} = a_{350} \cdot 10^{-6} \cdot exp(55.8 - \frac{16200}{SST}) \tag{5}$$

The parameterization for hydrolysis describes alkaline and acidic degradation of OCS by the reactions R1 and R2:

$$OCS + H_2O \rightarrow H_2S + CO_2 \tag{R1}$$

$$OCS + OH^- \rightarrow SH^- + CO_2 \tag{R2}$$

It was parameterized as a first order kinetic reaction including the rate constant k_h according to Eq. 6-8:

$$\frac{dC_{OCS}}{dt} = [OCS] \cdot k_h \tag{6}$$

$$k_h = exp(24.3 - \frac{10450}{SST}) + exp(22.8 - \frac{6040}{SST}) \cdot \frac{K}{a[H^+]} \tag{7}$$

$$-log_{10}K = \frac{3046.7}{SST} + 3.7685 + 0.0035486 \cdot \sqrt{SSS} \tag{8}$$

5   where a[H$^+$] is the proton activity and K the ion product of seawater(Dickinson and Riley, 1979).

Fluxes were calculated with Eq. 1 using the same parameterization for k_w as for the emission calculation from measurements described above.

The model input for simulations of the cruises OASIS and ASTRA-OMZ consisted of measurements made during the respective cruise, including SST and SSS (MicroCAT SBE41) measured every minute, CDOM absorption coefficient (spec-
10   trophotometrically measured ca. every 3 hours with a liquid capillary cell setup) and the ship's in situ measured meteorological data such as wind speed and global radiation averaged over 10 minutes (S-Fig. 1,2, S-Tab. 1,2). Forcing data was linearly interpolated to the time step of integration of 2 minutes.

For the global box model, monthly global meteorological fields with a spatial resolution of 2.8 x 2.8° were used (S-Tab. 3, S-Fig. 3). For global a$_{350}$ at the sea surface, monthly climatological means for absorption due to gelbstoff and detritus a$_4$43
15   from the MODIS-Aqua satellite (all available data, 2002-2014) (NASA, 2014) were corrected to 350 nm with Eq. 9 (Fichot and Miller, 2010; Launois et al., 2015a):

$$a_{350} = a_{443} \cdot exp(-0.02 \cdot (443 - 350)) \tag{9}$$

SST, wind speed, and atmospheric pressure were obtained as monthly climatological means from the same period, i.e. 2002 to 2014, by ERAInterim (Dee et al., 2011). A diel cycle of global radiation I was obtained by fitting the parable parameters a and
20   b during time of the day t in Eq. 10 (S-Fig. 4):

$$I = -a \cdot t^2 + b \tag{10}$$

to conditions of (i) x-axis interceptions in the distance of the sunshine duration and (ii) the integral being the daily incoming energy by ERAInterim (Dee et al., 2011). Monthly climatologies of mixed layer depths were used from the MIMOC project (Schmidtko et al., 2013). For details of data sources please refer to S-Tab. 1-3 provided in the supplementary material. The
25   time step of the model was set to 120 minutes, which had been tested to result in negligible (<3%) smoothing.

2.4   Assessing the indirect contribution of DMS with EMAC

Model output from the ECHAM/MESSy Atmospheric Chemistry (EMAC) from the simulation RC1SDbase-10a of the ES-CiMo project (Jöckel et al., 2015) are used to evaluate the contribution of DMS on the production of OCS. The model results were obtained with ECHAM5 version 5.3.02 and MESSy version 2.51, with a T42L90MA resolution (corresponding to a
30   quadratic Gaussian grid of approx. 2.8 by 2.8 ° in latitude and longitude) and 90 vertical hybrid pressure levels up to 0.01

hPa. The dynamics of the general circulation model were nudged by Newtonian relaxation towards ERA-Interim reanalysis data. DMS emissions were calculated with the AIRSEA submodel (Pozzer et al., 2006), which takes in account concentration of DMS in the atmosphere and in the ocean, following a two-layer conceptual model to calculate emissions (Liss and Slater, 1974). While atmospheric concentrations are estimated online by the model (with DMS oxidation), the oceanic concentrations

5   are prescribed as monthly climatologies (Lana et al., 2011). It was shown that such an online calculation of emissions provides the most realistic results when compared to measurements compared to a fixed emission rate (Lennartz et al., 2015). The on-line calculated concentration of DMS and OH have then been used to estimate the production of OCS. A production yield of 0.7% has been used for the reaction of DMS with OH (Barnes et al., 1994), using the reaction rate constant suggested by the International Union of Pure and Applied Chemistry (IUPAC) (Atkinson et al., 2004).

10   ## 3   Results and Discussion

3.1   Observations of OCS in the tropical ocean

OCS was measured in the surface ocean and the marine boundary layer (MBL) during three cruises in the tropics. Measurement locations (Fig. 1) include oligotrophic open ocean regions in the Indian Ocean (OASIS, 07-08/2014), open ocean and shelf areas in the eastern Pacific (ASTRA-OMZ, 10/2015) and a meridional transect in the Atlantic (TransPEGASO, 10-11/2014).

15   In the Indian and Pacific Oceans, continuous underway measurements provided the necessary temporal resolution to observe diel cycles of OCS concentrations in surface water. Dissolved OCS concentrations exhibited diel cycles with maxima 2 to 4 hours after local noon (Fig. 1), which are a consequence of photochemical production and removal by hydrolysis (Uher and Andreae, 1997a). OCS concentrations also varied spatially. Taking the absorption coefficient at 350 nm (a_{350}) as a proxy for CDOM content, daily mean OCS concentrations were higher in CDOM rich (Tab. 3, 28.3±19.7 pmol OCS L^{-1}, a_{350}:

20   0.15±0.03 m^{-1}) than in CDOM poor waters (Tab. 3, OASIS: 9.1±3.5 pmol OCS L^{-1}, a_{350}: 0.03±0.02 m^{-1}). Samples during TransPEGASO were measured with gas chromatography/mass spectrometry twice a day (around 8-10 and 15-17 h local times). Therefore, the full diel cycles could not be reconstructed and potential variations of OCS with CDOM absorption were overlaid by diel variations. Nevertheless, the observed range of OCS concentrations in the Atlantic corresponds well to the observations from the eastern Pacific and Indian Ocean (Tab 3), and is consistent with measurements from a previous Atlantic meridional

25   transect (AMT-7) cruise (Kettle et al., 2001) (1.3-112.0 pmol OCS L^{-1}, mean 21.7 pmol OCS L^{-1}).

Air-sea fluxes calculated from surface concentrations and mixing ratios of OCS as a function of wind speed generally follow the diel cycle of the surface ocean concentration. While supersaturation prevailed during the day, low nighttime concentrations usually led to oceanic uptake of atmospheric OCS. OCS fluxes integrated over one day ranged from -0.024 to -0.0002 g S km^{-2} in the open Indian Ocean and from 0.38 to 2.7 g S km^{-2} in the coastal Pacific. During the observed periods, the ocean was a

30   net sink of atmospheric OCS in the Indian Ocean, whereas it was a net source in the eastern Pacific. Although an assessment of net flux is difficult given the lower temporal resolution during TransPEGASO, calculated emissions were in the same range as the ones measured in the Pacific and Indian Ocean. Together, they likely constrain the variability of OCS emissions in the

tropics. Our observed concentrations and calculated emissions are approximately one order of magnitude lower than the annual mean surface concentrations and emissions simulated in the 3D global ocean model NEMO-PISCES (Launois et al., 2015a).

3.2 A direct global oceanic emission estimate for OCS

Our OCS observations from the Indian and Pacific Ocean were used to improve a box model for simulating OCS concentrations in the surface ocean (Kettle, 2002; Uher and Andreae, 1997b; von Hobe et al., 2003) that includes air-sea exchange (Nightingale et al., 2000), photoproduction, light-independent production (Von Hobe et al., 2001), and hydrolysis(Elliott et al., 1989).

Following an earlier study (von Hobe et al., 2003), we use our observations to optimize the photoproduction rate constant p in an inverse set-up of the box model, considering only periods of sunlight in homogeneous water masses (Fig. 2, blue lines). The optimized p and the mean a_{350} (as a proxy for CDOM absorption) for each fitting period as well as p-a_{350} pairs from a previous study in the Atlantic (von Hobe et al., 2003) are used to derive a linear relationship (R^2=0.71, Fig. 3) that was found to reproduce the temporal variability of OCS during our cruises in the Indian and Pacific Oceans rather well when used in the forward mode of the model (Fig. 2, black lines). The general overestimation of observed concentrations in both the Indian Ocean (observed mean concentration: 9.1±3.5 pmol L^{-1}; simulated: 10.8±3.9 pmol L^{-1}) and more pronounced in the eastern Pacific (observed mean: 28.3±19.7 pmol L^{-1}; simulated: 47.3±25.4 pmol L^{-1}) can largely be attributed to a lack of downward mixing inherent in the mixed layer box model due to the assumption of the OCS concentration being constant throughout the entire mixed layer.

Using the linear p-a_{350} parameterization for the first time in a global model, the same box model as for the case studies is applied to estimate sea surface concentrations and fluxes of OCS on a global scale (Fig. 4). The OCS production is consistent with the global distribution of CDOM absorption (S-Fig. 5) with highest concentrations calculated for coastal regions and higher latitudes. Despite the photochemical hotspot in the tropics (30°N-30°S), degradation by hydrolysis prevents any accumulation of OCS in the surface water, as we calculated the lifetime due to hydrolysis to be only 7 hours (S-Fig. 5). The simulated range of water concentrations is too low to sustain emissions in the tropics that could close the atmospheric budget of OCS (Fig. 4). Integrated over one year, the tropical ocean (30°N-30°S) is even a small net sink of -3.0 Gg S yr^{-1}. Globally, the integration over one year yields annual oceanic OCS emissions of 130 Gg S. Our results corroborate the upper limit of an earlier study that used an observation-derived emission inventory (Tab. 1) (Kettle, 2002). Compared to the model used in that study, our box model study has a more process oriented physical basis; in particular p depends on a_{350} derived from observations in different regions. Clearly, our results contradict the latest bottom-up emission estimate from the NEMO-PISCES model(Launois et al., 2015a) and do not support the finding from top-down (Suntharalingam et al., 2008; Berry et al., 2013; Kuai et al., 2015; Glatthor et al., 2015; Launois et al., 2015a) approaches that the missing OCS source can be ascribed to direct emissions from the ocean, either tropical or global.

Simulated concentrations and fluxes carry some uncertainties from input parameters and the gas-exchange parameterization. One major uncertainty associated with the mixed-layer box model approach arises from the fact that it does not adequately account for downward mixing and vertical concentration gradients within the mixed layer. Under most circumstances, and especially in the tropical open ocean, where hydrolysis greatly exceeds surface outgassing and low a_{350} makes photoproduction

extend further down in the water column, the model tends to overestimate the real OCS concentrations, as was shown for our two cruises above. Therefore, we deem the fluxes from our global simulation to represent an upper limit of the true fluxes. Only at high latitudes would we expect more complex uncertainties, because hydrolysis at low temperatures is slow and only photoproduction and loss by outgassing are directly competing at the very surface. Nevertheless, even at high latitudes OCS

5 concentrations in our global simulation are in the same range as past observations (Ulshöfer et al., 1995; Uher and Andreae, 1997a).

3.3 Indirect tropical OCS emissions by DMS and CS_2

A significant contribution to the OCS budget in the atmosphere results from oceanic emissions of DMS and CS_2 that are partially converted to OCS on time scales of hours to days (Chin and Davis, 1993; Watts, 2000; Kettle, 2002). A yield of 0.7

10 % for OCS is used for the reaction of DMS with OH (Barnes et al., 1994), which results in a mean indirect OCS source of 80 (65 - 110) Gg S yr^{-1} from the global ocean. However, the formation of OCS from DMS involves a complex multi-step reaction mechanism that is far from being fully understood. It has been shown in laboratory experiments, that the presence of NO_x reduces the OCS yield considerably (Arsene et al., 2001), which would make our indirect emission estimate based on the yield of 0.7% an upper limit. However, the yield was measured under laboratory conditions, and may be different and

15 more variable under natural conditions. Better constraining the OCS yield of DMS is thus crucial to reduce uncertainties in the indirect emission estimate.

For CS_2, the atmospheric reaction pathway producing OCS is better understood with a well constrained molar conversion ratio of 0.81 (Chin and Davis, 1993). However, the global distribution of oceanic CS_2 concentration, hence its emissions to the atmosphere, are poorly known. Few field studies reported CS_2 in the surface ocean (Kim and Andreae, 1992; Xie and

20 Moore, 1999), with evidence for photochemical production (Xie et al., 1998) as well as for a biological source (Xie et al., 1999). In our study, surface CS_2 concentrations (S-Fig. 6) were on average 17.8±8.9 pmol L^{-1} during ASTRA-OMZ, and 62.5±42.1 pmol L^{-1} during TransPEGASO (Tab. 3). The latter values are higher than previously reported concentrations from the AMT-7 cruise in the central Atlantic (Kettle et al., 2001) (10.9±15.2 pmol L^{-1}). We extrapolate a weighted mean of the CS_2 emissions from TransPEGASO (n=42, 13.7±9.8 g S d^{-1} km^{-2}), ASTRA-OMZ (n=122, 4.1±3.2 g S d^{-1} km-2) and

25 AMT-7 (Kettle et al., 2001) (n=744, 1.6±1.8 g S d^{-1} km^{-2}) in order to estimate CS_2 derived OCS emissions from the global ocean. According to our extrapolation, 135 (7-260) Gg S yr^{-1} enter the atmosphere as oceanic CS_2 emissions converted to OCS. This number agrees with previous estimates and is also lower than the missing source of OCS.

For oceanic emission estimates used to constrain GPP, quantifying the seasonal cycle of the single contributors is essential. For example, high emissions during oceanic spring and fall blooms could mask OCS uptake by the terrestrial vegetation, and

30 therefore neglecting them could lead to an underestimation of global GPP, with implications for the atmospheric and terrestrial carbon budget.

4 Conclusions

Considering the observational evidence and the modelled global emission estimate of 130 Gg S yr^{-1}, direct OCS emissions from the oceans are too low to account for the missing source. Together with indirect emissions, the oceanic source strength of OCS adds up to 345 Gg S yr^{-1} compared to 465-1089 Gg S yr^{-1} required to balance the suggested increase of vegetation

5   uptake. Hence, direct and indirect oceanic emissions of OCS are unlikely to balance the budget after the upward revision of the vegetation sink.

To resolve this imbalance, top-down and bottom-up derived emission inventories have to be brought to agreement. On one hand, given the large range of the suggested missing source of 235-800 Gg S yr^{-1}, reducing the uncertainty in inverse estimates would help to better constrain the likelihood of such a large gap in the atmospheric budget. As our study suggests, the search

10   for an additional source of OCS to the atmosphere should focus on other sources than oceanic emissions. There are indications of other parts of the OCS budget such as domestic coal combustion, are currently underestimated (Du et al., 2016).

On the other hand, a redistribution of the magnitude and seasonality of known sources and sinks could also bring top-down and bottom-up estimates into agreement, making the missing source at least partly obsolete. For example, the general view of oxic soils as a sink for OCS has recently been challenged. Field (Maseyk et al., 2014; Billesbach et al., 2014) and incubation

15   studies (Whelan et al., 2016) show that some oxic soils may shift from OCS uptake to emission depending on the temperature and water content. The role of soils, especially in warmer regions such as the tropics would be worth reevaluating. Furthermore, it has been speculated previously that vegetation uptake might not be solely responsible for the decrease in OCS mixing ratios in fall, because of the temporal lag between CO_2 and OCS minimum (Montzka et al., 2007). The observed seasonality in mixing ratios is a superposition of the seasonality of all individual sources and sinks. These seasonalities are currently neglected or

20   associated with a considerable uncertainty. An improved understanding of the seasonality of the individual sources and sinks could be sufficient to reproduce observations without increasing the vegetation sink. This would balance the resulting gap in the budget without requiring an additional ocean source. First steps to resolve OCS seasonality in sources and sinks are currently undertaken, e.g. in the case of anthropogenic emissions (Campbell et al., 2015).

All in all, better constraints on the seasonality and magnitude of the atmospheric OCS sources and sinks are critical for a

25   better assessment of the role of this compound in climate and its application to quantify GPP on a global scale. This study confirms oceanic emission as the largest known single source of atmospheric OCS, but shows that its magnitude is not enough to balance the suggested increased vegetation sink.

Appendix A: List of parameters

Symbol	Meaning
a_{350}	absorption coefficient of CDOM at 350nm
a	fitted parameter in diurnal cycle of I
b	fitted parameter in diurnal cycle of I
c_{air}	concentration in air
C_{OCS}	concentration of OCS in wtaer
F	gas flux
H	Henry constant
I	downwelling solar radiation
K	ion product of seawater
k_w	water side transfer velocity in air-sea gas exchange
MLD	mixed layer depth
p	photoproduction rate constant
SSS	sea surface salinity
SST	sea surface temperature
Sc	Schmidt number
t	time
θ	zenith angle
u_{10}	wind speed at 10m height
UV	ultra violett radiation
z	depth

Acknowledgements. We thank the captain and crew of the research vessels SONNE I and II as well as HESPERIDES for assistance during the cruises SO235-OASIS (BMBF - FK03G0235A), SO243-ASTRA-OMZ (BMBF - FK03G0243A) and TransPEGASO. We thank

5   H.W. Bange and A. Körtzinger for providing equipment for the continuous underway system and C. Schlundt for support during CS_2 measurements. This work was supported by the German Federal Ministry of Education and Research through the project ROMIC-THREAT (BMBF-FK01LG1217A and 01LG1217B) and ROMIC- SPITFIRE (BMBF- FKZ: 01LG1205C). Additional funding for C.A.M. and S.T.L. came from the Helmholtz Young Investigator Group of C.A. M., TRASE-EC (VH-NG-819), from the Helmholtz Association through the President's Initiative and Networking Fund and the GEOMAR Helmholtz-Zentrum für Ozeanforschung Kiel. K.K. acknowledges financial

10 support from StratoClim (603557), and P.C. and R.S. acknowledge support from Spanish MINECO through PEGASO (CTM2012-37615). We gratefully acknowledge the data provided by ECMWF (ERAInterim) and NASA (MODIS Aqua). DKRZ and its scientific steering committee are gratefully acknowledged for providing the HPC and data archiving resources for this consortial project ESCiMo (Earth System Chemistry Integrated Modelling). E.A. acknowledges support from NASA Upper Atmosphere Research Program.

References

Andreae, M. O. and Ferek, R.: Photochemical production of carbonyl sulfide in seawater and its emission to the atmosphere, Global Biogeo-chemical Cycles, 6, 175–183, 2002.

Arneth, A., Harrison, S. P., Zaehle, S., Tsigaridis, K., Menon, S., Bartlein, P. J., Feichter, J., Korhola, A., Kulmala, M., O'Donnell, D.,
5   Schurgers, G., Sorvari, S., and Vesala, T.: Terrestrial biogeochemical feedbacks in the climate system, Nature Geoscience, 3, 525–532, 2010.

Arsene, C., Barnes, I., Becker, K. H., and Mocanu, R.: FT-IR product study on the photo-oxidation of dimethyl sulphide in the presence of NOx - temperature dependence, Atmospheric Environment, 35, 3769–3780, times Cited: 39, 2001.

Arévalo-Martínez, D. L., Beyer, M., Krumbholz, M., Piller, I., Kock, A., Steinhoff, T., Körtzinger, A., and Bange, H. W.: A new method for
10   continuous measurements of oceanic and atmospheric N2O, CO and CO2: performance of off-axis integrated cavity output spectroscopy (OA-ICOS) coupled to non-dispersive infrared detection (NDIR), Ocean Sci., 9, 1071–1087, oS, 2013.

Asaf, D., Rotenberg, E., Tatarinov, F., Dicken, U., Montzka, S. A., and Yakir, D.: Ecosystem photosynthesis inferred from measurements of carbonyl sulphide flux, Nature Geoscience, 6, 186–190, 2013.

Asher, W. E. and Wanninkhof, R.: The effect of bubble-mediated gas transfer on purposeful dual-gaseous tracer experiments, Journal of
15   Geophysical Research: Oceans, 103, 10 555–10 560, 1998.

Atkinson, R., Baulch, D. L., Cox, R. A., Crowley, J. N., Hampson, R. F., Hynes, R. G., Jenkin, M. E., Rossi, M. J., and Troe, J.: Evaluated kinetic and photochemical data for atmospheric chemistry: Volume I - gas phase reactions of Ox, HOx, NOx and SOx species, Atmos. Chem. Phys., 4, 1461–1738, aCP, 2004.

Barnes, I., Becker, K. H., and Patroescu, I.: The tropospheric oxidation of dimethyl sulfide: A new source of carbonyl sulfide, Geophysical
20   Research Letters, 21, 2389–2392, 1994.

Beer, C., Reichstein, M., Tomelleri, E., Ciais, P., Jung, M., Carvalhais, N., Rödenbeck, C., Arain, M. A., Baldocchi, D., and Bonan, G. B.: Terrestrial gross carbon dioxide uptake: global distribution and covariation with climate, Science, 329, 834–838, 2010.

Berry, J., Wolf, A., Campbell, J. E., Baker, I., Blake, N., Blake, D., Denning, A. S., Kawa, S. R., Montzka, S. A., Seibt, U., Stimler, K., Yakir, D., and Zhu, Z.: A coupled model of the global cycles of carbonyl sulfide and CO2: A possible new window on the carbon cycle, Journal
25   of Geophysical Research: Biogeosciences, 118, 842–852, 2013.

Billesbach, D. P., Berry, J. A., Seibt, U., Maseyk, K., Torn, M. S., Fischer, M. L., Abu-Naser, M., and Campbell, J. E.: Growing season eddy covariance measurements of carbonyl sulfide and CO2 fluxes: COS and CO2 relationships in Southern Great Plains winter wheat, Agricultural and Forest Meteorology, 184, 48–55, 2014.

Brühl, C., Lelieveld, J., Crutzen, P. J., and Tost, H.: The role of carbonyl sulphide as a source of stratospheric sulphate aerosol and its impact
30   on climate, Atmos. Chem. Phys., 12, 1239–1253, aCP, 2012.

Campbell, J. E., Carmichael, G. R., Chai, T., Mena-Carrasco, M., Tang, Y., Blake, D. R., Blake, N. J., Vay, S. A., Collatz, G. J., Baker, I., Berry, J. A., Montzka, S. A., Sweeney, C., Schnoor, J. L., and Stanier, C. O.: Photosynthetic Control of Atmospheric Carbonyl Sulfide During the Growing Season, Science, 322, 1085–1088, times Cited: 44, 2008.

Campbell, J. E., Whelan, M. E., Seibt, U., Smith, S. J., Berry, J. A., and Hilton, T. W.: Atmospheric carbonyl sulfide sources from anthro-
35   pogenic activity: Implications for carbon cycle constraints, Geophysical Research Letters, 42, 3004–3010, 2015.

Chin, M. and Davis, D. D.: Global sources and sinks of OCS and CS2 and their distributions, Global Biogeochemical Cycles, 7, 321–337, 1993.

Crutzen, P. J.: The possible importance of CSO for the sulfate layer of the stratosphere, Geophysical Research Letters, 3, 73–76, 1976.

De Bruyn, W., Swartz, E., Hu, J., Shorter, J., Davidovits, P., Worsnop, D., Zahniser, M., and Kolb, C.: Henrys law solubilities and Setcheniw coefficients for biogenic reduced sulphur species obtained from gas-liquid uptake measurements, Journal of Geophysical Research Atmosphere, 100, 7245–7251, 1995.

de Gouw, J. A., Warneke, C., Montzka, S. A., Holloway, J. S., Parrish, D. D., Fehsenfeld, F. C., Atlas, E. L., Weber, R. J., and Flocke, F. M.: Carbonyl sulfide as an inverse tracer for biogenic organic carbon in gas and aerosol phases, Geophysical Research Letters, 36, 2009.

Dee, D. P., Uppala, S. M., Simmons, A. J., Berrisford, P., Poli, P., Kobayashi, S., Andrae, U., Balmaseda, M. A., Balsamo, G., Bauer, P., Bechtold, P., Beljaars, A. C. M., van de Berg, L., Bidlot, J., Bormann, N., Delsol, C., Dragani, R., Fuentes, M., Geer, A. J., Haimberger, L., Healy, S. B., Hersbach, H., Hólm, E. V., Isaksen, L., Kållberg, P., Köhler, M., Matricardi, M., McNally, A. P., Monge-Sanz, B. M., Morcrette, J. J., Park, B. K., Peubey, C., de Rosnay, P., Tavolato, C., Thépaut, J. N., and Vitart, F.: The ERA-Interim reanalysis: configuration and performance of the data assimilation system, Quarterly Journal of the Royal Meteorological Society, 137, 553–597, 2011.

Dickinson, A. G. and Riley, J.: The estimation of acid dissociation constants in seawater media from potentiometric titrations with strong base, Mar. Chem., 7, 89–99, 1979.

Du, Q., Zhang, C., Mu, Y., Cheng, Y., Zhang, Y., Liu, C., Song, M., Tian, D., Liu, P., Liu, J., Xue, C., and Ye, C.: An important missing source of atmospheric carbonyl sulfide: Domestic coal combustion, Geophysical Research Letters, pp. n/a–n/a, 2016.

Elliott, S., Lu, E., and Rowland, F. S.: Rates and mechanisms for the hydrolysis of carbonyl sulfide in natural waters, Environmental Science & Technology, 23, 458–461, 1989.

Ferek, R. and Andreae, M. O.: The supersaturation of carbonyl sulfide in surface waters of the pacific oceans off Peru, Geophysical Research Letters, 10, 393–395, 1983.

Ferek, R. and Andreae, M. O.: Photochemical production of carbonyl sulphide in marine surface waters, Letters to Nature, 1984, 148–150, 1984.

Fichot, C. G. and Miller, W. L.: An approach to quantify depth-resolved marine photochemical fluxes using remote sensing: Application to carbon monoxide (CO) photoproduction, Remote Sensing of Environment, 114, 1363–1377, 2010.

Flöck, O. R., Andreae, M. O., and Dräger, M.: Environmentally relevant precursors of carbonyl sulfide in aquatic systems, Marine Chemistry, 59, 71–85, 1997.

Glatthor, N., Höpfner, M., Baker, I. T., Berry, J., Campbell, J. E., Kawa, S. R., Krysztofiak, G., Leyser, A., Sinnhuber, B. M., Stiller, G. P., Stinecipher, J., and Clarmann, T. v.: Tropical sources and sinks of carbonyl sulfide observed from space, Geophysical Research Letters, 2015.

Hayduk, W. and Laudie, H.: Prediction of diffusion coefficients for nonelectrolytes in dilute aqueous solutions, AIChE Journal, 20, 611–615, 1974.

Jöckel, P., Tost, H., Pozzer, A., Kunze, M., Kirner, O., Brenninkmeijer, C. A. M., Brinkop, S., Cai, D. S., Dyroff, C., Eckstein, J., Frank, F., Garny, H., Gottschaldt, K. D., Graf, P., Grewe, V., Kerkweg, A., Kern, B., Matthes, S., Mertens, M., Meul, S., Neumaier, M., Nützel, M., Oberländer-Hayn, S., Ruhnke, R., Runde, T., Sander, R., Scharffe, D., and Zahn, A.: Earth System Chemistry Integrated Modelling (ESCiMo) with the Modular Earth Submodel System (MESSy, version 2.51), Geosci. Model Dev. Discuss., 2015, 8635–8750, gMDD, 2015.

Johnson, J. E. and Harrison, H.: Carbonyl Sulfide Concentrations in the Surface Waters and Above the Pacific Ocean, Journal of Geophysical Research, 91, 7883–7888, 1986.

Kettle, A. J.: Global budget of atmospheric carbonyl sulfide: Temporal and spatial variations of the dominant sources and sinks, Journal of Geophysical Research, 107, 2002.

Kettle, A. J., Rhee, T. S., von Hobe, M., Poulton, A., Aiken, J., and Andreae, M. O.: Assessing the flux of different volatile sulfur gases from the ocean to the atmosphere, Journal of Geophysical Research: Atmospheres, 106, 12 193–12 209, 2001.

Kim, K. H. and Andreae, M. O.: Carbon disulfide in the estuarine, coastal and oceanic environments, Marine Chemistry, 40, 179–197, 1992.

Kremser, S., Jones, N. B., Palm, M., Lejeune, B., Wang, Y., Smale, D., and Deutscher, N. M.: Positive trends in Southern Hemisphere carbonyl sulfide, Geophysical Research Letters, 42, 9473–9480, 2015.

Kremser, S., Thomason, L. W., von Hobe, M., Hermann, M., Deshler, T., Timmreck, C., Toohey, M., Stenke, A., Schwarz, J. P., Weigel, R., Fueglistaler, S., Prata, F. J., Vernier, J.-P., Schlager, H., Barnes, J. E., Antuña-Marrero, J.-C., Fairlie, D., Palm, M., Mahieu, E., Notholt, J., Rex, M., Bingen, C., Vanhellemont, F., Bourassa, A., Plane, J. M. C., Klocke, D., Carn, S. A., Clarisse, L., Trickl, T., Neely, R., James, A. D., Rieger, L., Wilson, J. C., and Meland, B.: Stratospheric aerosol—Observations, processes, and impact on climate, Reviews of Geophysics, 54, 2016.

Kuai, L., Worden, J. R., Campbell, J. E., Kulawik, S. S., Li, K.-F., Lee, M., Weidner, R. J., Montzka, S. A., Moore, F. L., Berry, J. A., Baker, I., Denning, A. S., Bian, H., Bowman, K. W., Liu, J., and Yung, Y. L.: Estimate of carbonyl sulfide tropical oceanic surface fluxes using Aura Tropospheric Emission Spectrometer observations, Journal of Geophysical Research: Atmospheres, 120, 11,012–11,023, 2015.

Lana, A., Bell, T. G., Simo, R., Vallina, S. M., Ballabrera-Poy, J., Kettle, A. J., Dachs, J., Bopp, L., Saltzman, E. S., Stefels, J., Johnson, J. E., and Liss, P. S.: An updated climatology of surface dimethlysulfide concentrations and emission fluxes in the global ocean, Global Biogeochemical Cycles, 25, times Cited: 55, 2011.

Launois, T., Belviso, S., Bopp, L., Fichot, C. G., and Peylin, P.: A new model for the global biogeochemical cycle of carbonyl sulfide - Part 1: Assessment of direct marine emissions with an oceanic general circulation and biogeochemistry model, Atmos. Chem. Phys., 15, 2295–2312, aCP, 2015a.

Launois, T., Peylin, P., Belviso, S., and Poulter, B.: A new model of the global biogeochemical cycle of carbonyl sulfide – Part 2: Use of carbonyl sulfide to constrain gross primary productivity in current vegetation models, Atmos. Chem. Phys., 15, 9285–9312, aCP, 2015b.

Lennartz, S. T., Krysztofiak, G., Marandino, C. A., Sinnhuber, B. M., Tegtmeier, S., Ziska, F., Hossaini, R., Krüger, K., Montzka, S. A., Atlas, E., Oram, D. E., Keber, T., Bönisch, H., and Quack, B.: Modelling marine emissions and atmospheric distributions of halocarbons and dimethyl sulfide: the influence of prescribed water concentration vs. prescribed emissions, Atmos. Chem. Phys., 15, 11 753–11 772, aCP, 2015.

Liss, P. S. and Slater, P. G.: Flux of gases across air-sea interface, Nature, 247, 181–184, times Cited: 897, 1974.

Maseyk, K., Berry, J. A., Billesbach, D., Campbell, J. E., Torn, M. S., Zahniser, M., and Seibt, U.: Sources and sinks of carbonyl sulfide in an agricultural field in the Southern Great Plains, Proceedings of the National Academy of Sciences of the United States of America, 111, 9064–9069, times Cited: 8, 2014.

McGillis, W. R., Edson, J. B., Hare, J. E., and Fairall, C. W.: Direct covariance air-sea CO2 fluxes, Journal of Geophysical Research-Oceans, 106, 16 729–16 745, times Cited: 120, 2001.

Mihalopoulos, N., Nguyen, B. C., Putaud, J. P., and Belviso, S.: The oceanic source of carbonyl sulfide (COS), Atmospheric Environment, 26A, 1383–1394, 1992.

Miller, S., Marandino, C., De Bruyn, W., and Saltzman, E. S.: Air-sea gas exchange of CO2 and DMS in the North Atlantic by eddy covariance, Geophysical Research Letters, 36, 2009.

Montzka, S. A., Calvert, P., Hall, B. D., Elkins, J. W., Conway, T. J., Tans, P. P., and Sweeney, C.: On the global distribution, seasonality, and budget of atmospheric carbonyl sulfide (COS) and some similarities to CO2, Journal of Geophysical Research, 112, 2007.

Najjar, R., Erickson, D., and Madronich, S.: Modeling the air-sea fluxes of gases formed from the decomposition of dissolved organic matter: Carbonyl sulfide and carbon monoxide, pp. 107–132, John Wiley & Sons, 1995.

5 NASA: MODIS-Aqua Ocean Color Data, 2014.

Nightingale, P. D., Malin, G., Law, C. S., Watson, A. J., Liss, P. S., Liddicoat, M. I., Boutin, J., and Upstill-Goddard, R. C.: In situ evaluation of air-sea gas exchange parameterizations using novel conservative and volatile tracers, Global Biogeochemical Cycles, 14, 373–387, times Cited: 526, 2000.

Notholt, J., Kuang, Z., Rinsland, C. P., Toon, G. C., Rex, M., Jones, N., Albrecht, T., Deckelmann, H., Krieg, J., Weinzierl, C., Bingemer,

10 H., Weller, R., and Schrems, O.: Enhanced Upper Tropical Tropospheric COS: Impact on the Stratospheric Aerosol Layer, Science, 300, 307–310, 2003.

Pozzer, A., Jöckel, P., Sander, R., Williams, J., Ganzeveld, L., and Lelieveld, J.: Technical Note: The MESSy-submodel AIRSEA calculating the air-sea exchange of chemical species, Atmos. Chem. Phys., 6, 5435–5444, aCP, 2006.

Rasmussen, R. A., Khalil, M. A. K., and Hoyt, S. D.: The oceanic source of carbonyl sulfide (OCS), Atmospheric Environment, 16, 1591–

15 1594, 1982.

Schauffler, S. M., Atlas, E. L., Flocke, F., Lueb, R. A., Stroud, V., and Travnicek, W.: Measurements of bromine containing organic compounds at the tropical tropopause, Geophysical Research Letters, 25, 317–320, times Cited: 56, 1998.

Schmidtko, S., Johnson, G. C., and Lyman, J. M.: MIMOC: A global monthly isopycnal upper-ocean climatology with mixed layers, Journal of Geophysical Research-Oceans, 118, 1658–1672, 2013.

20 Schrade, S.: Ground based measurements of Carbon Dioxide and other climatically relevant trace gases using Off-Axis Integrated-Cavity-Output-Spectroscopy (ICOS), Ph.D. thesis, 2011.

Sikorski, R. J. and Zika, R. G.: Modeling mixed-layer photochemistry of H2O2: Optical and chemical modeling of production, Journal of Geophysical Research: Oceans, 98, 2315–2328, 1993.

Stefels, J., Steinke, M., Turner, S., Malin, G., and Belviso, S.: Environmental constraints on the production and removal of the climatically

25 active gas dimethylsulphide (DMS) and implications for ecosystem modelling, Biogeochemistry, 83, 245–275, 2007.

Suntharalingam, P., Kettle, A. J., Montzka, S. M., and Jacob, D. J.: Global 3-D model analysis of the seasonal cycle of atmospheric carbonyl sulfide: Implications for terrestrial vegetation uptake, Geophysical Research Letters, 35, L19 801, 2008.

Turco, R. P., Whitten, R. C., Toon, O. B., Pollack, J. B., and Hamill, P.: OCS, stratospheric aerosols and climate, Nature, 283, 283–285, 10.1038/283283a0, 1980.

30 Uher, G. and Andreae, M. O.: The diel cycle of carbonyl sulfide in marine surface waters: field study results and a simple model, Atmospheric Geochemistry, 2, 313–344, 1997a.

Uher, G. and Andreae, M. O.: Photochemical production of carbonyl sulfide in North Sea water: A process study, Limnology and Oceanography, 42, 432–442, 1997b.

Ulshöfer, V. and Andreae, M. O.: Carbonyl Sulfide (COS) in the Surface Ocean and the Atmospheric COS Budget, Atmospheric Geochem-

35 istry, 3, 283–303, 1998.

Ulshöfer, V., Uher, G., and Andreae, M. O.: Evidence for a winter sink of atmospheric carbonyl sulfide in the northeast Atlantic Ocean, Geophysical Research Letters, 22, 2601–2604, 1995.

Von Hobe, M., Cutter, G. A., Kettle, A. J., and Andreae, M. O.: Dark production: A significant source of oceanic COS, Journal of Geophysical Research, 106, 31 217, 2001.

von Hobe, M., Najjar, R., Kettle, A., and Andreae, M.: Photochemical and physical modeling of carbonyl sulfide in the ocean, Journal of Geophysical Research, 108, 2003.

5 Wanninkhof, R., Asher, W. E., Ho, D. T., Sweeney, C., and McGillis, W. R.: Advances in Quantifying Air-Sea Gas Exchange and Environmental Forcing, Annual Review of Marine Science, 1, 213–244, 2009.

Watts, S. F.: The mass budgets of carbonyl sulfide, dimethyl sulfide, carbon disulfide and hydrogen sulfide, Atmospheric Environment, 34, 761–779, 2000.

Weiss, P., Andrews, S., Johnson, J. E., and Zafiriou, O.: Photoproduction of carbonyl sulfide in south Pacific Ocean waters as a function of

10 irradiation wavelength, Geophysical Research Letters, 22, 215–218, 1995a.

Weiss, P., Johnson, J. E., Gammon, R., and Bates, T.: Reevaluation of the open ocean source of carbonyl sulfide to the atmosphere, Journal of Geophysical Research, 100, 23 083–23 092, 1995b.

Whelan, M. E., Hilton, T. W., Berry, J. A., Berkelhammer, M., Desai, A. R., and Campbell, J. E.: Carbonyl sulfide exchange in soils for better estimates of ecosystem carbon uptake, Atmos. Chem. Phys., 16, 3711–3726, aCP, 2016.

15 Xie, H. and Moore, R. M.: Carbon disulfide in the North Atlantic and Pacific oceans, Journal of Geophysical Research, 104, 5393, 1999.

Xie, H., Moore, R. M., and Miller, W. L.: Photochemical production of carbon disulphide in seawater, Journal of Geophysical Research: Oceans, 103, 5635–5644, 1998.

Xie, H., Scarratt, M. G., and Moore, R. M.: Carbon disulphide production in laboratory cultures of marine phytoplankton, Atmospheric Environment, 33, 3445–3453, 1999.

20 Xu, X., Bingemer, H. G., Georgii, H. W., Schmidt, U., and Bartell, U.: Measurements of carbonyl sulfide (COS) in surface seawater and marine air, and estimates of the air-sea flux from observations during two Atlantic cruises, Journal of Geophysical Research, 106, 3491, 2001.
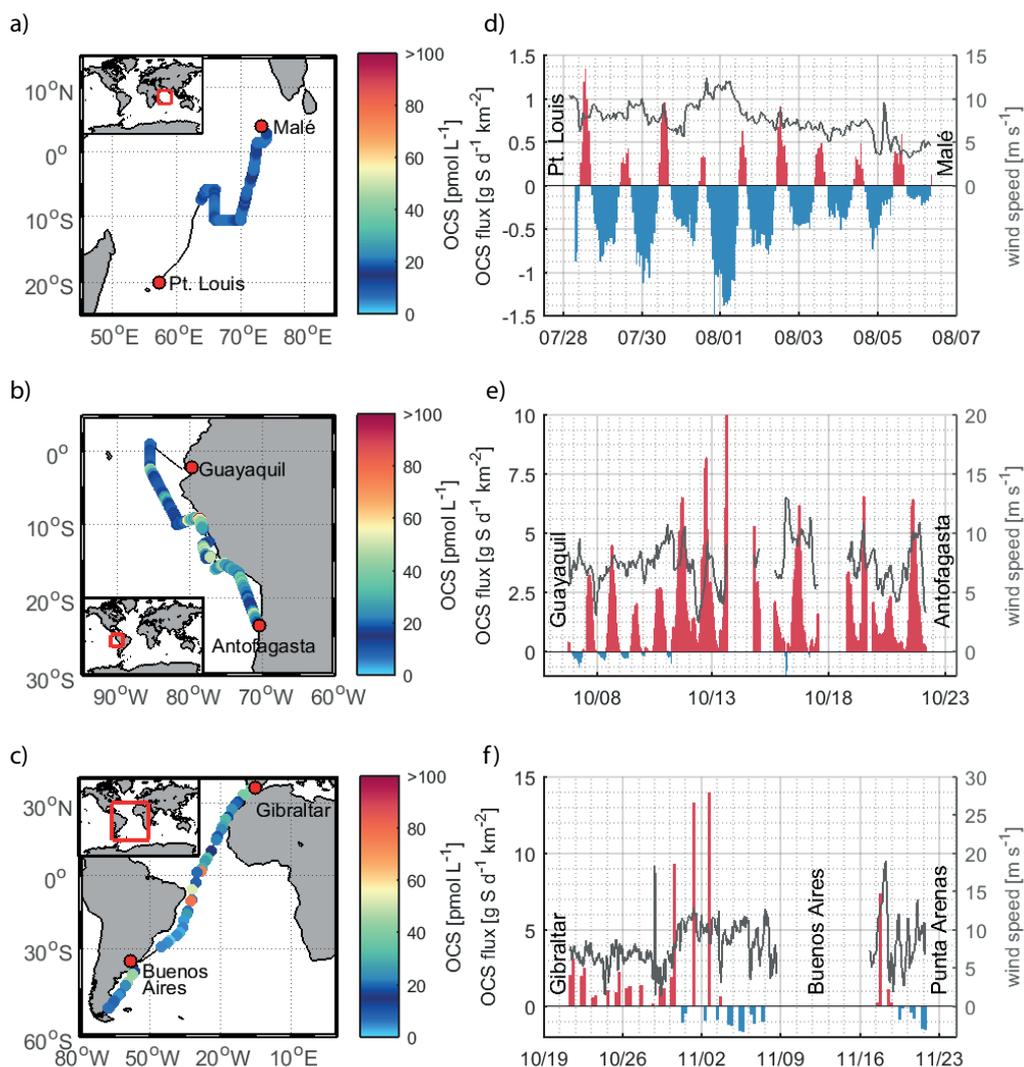
Figure 1. Observed OCS water concentrations and calculated emissions: Observations of OCS concentrations in the surface ocean during three cruises a) OASIS, b) ASTRA-OMZ, and c) TransPEGASO; and the corresponding emissions calculated based on the concentration gradient between water and marine boundary layer (d-f). Outgassing is indicated in red bars; oceanic uptake in blue bars. The grey line shows wind speed measured onboard the vessels. Flux data are shown with different scales on the y-axes. Data gaps occurred during stays in port and territorial waters or during instrument tests.
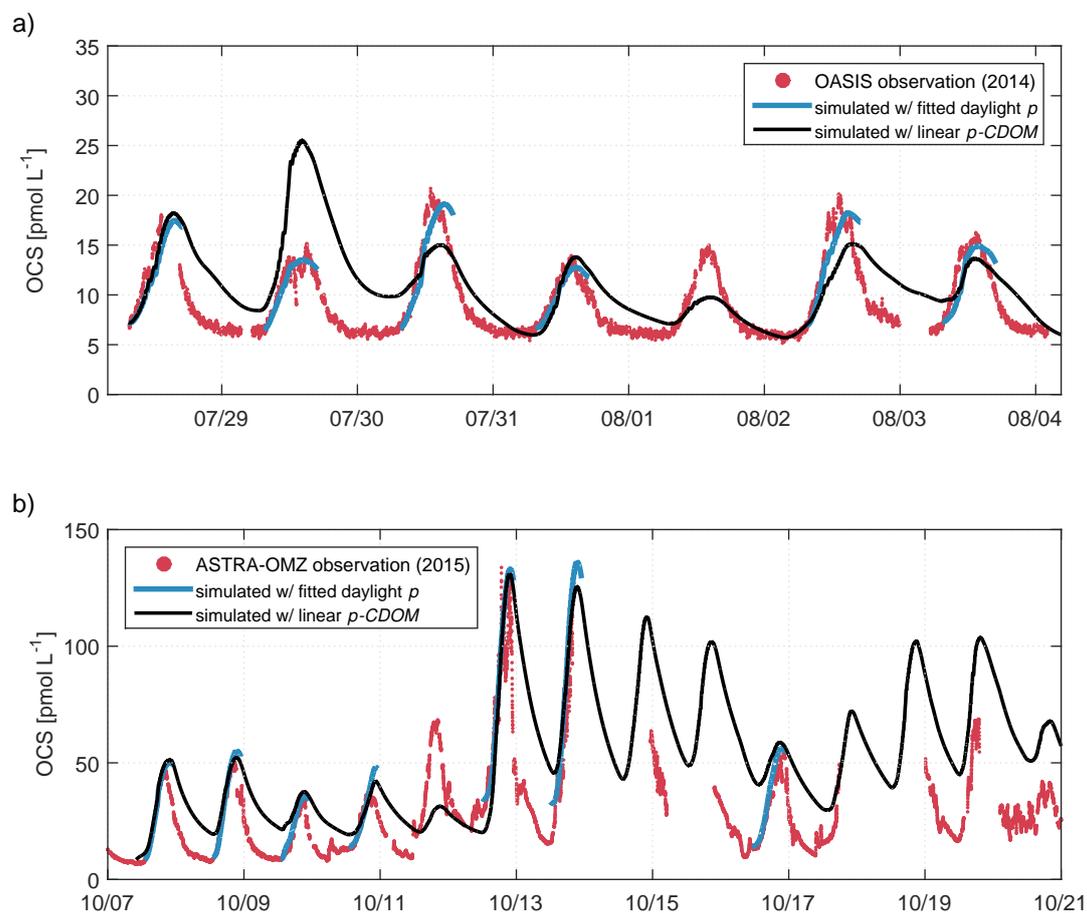
Figure 2. Box model simulations compared to observations: Comparison of simulated OCS water concentrations against measurements from the OASIS cruise to the Indian Ocean (a) and the eastern Pacific Ocean during the ASTRA-OMZ cruise (b). Blue indicates OCS concentrations with a least-square fit for the photoproduction rate constant p during daylight, fitted individually for days with homogeneous water masses (SST, a_{350}). Black shows the simulation including the p depending on a_{350}, obtained from linear regression of individually fitted p with a_{350} (R^2=0.71). The time on the x-axis is local time (GMT+5 during OASIS 2014, GMT-4 during ASTRA-OMZ 2015).
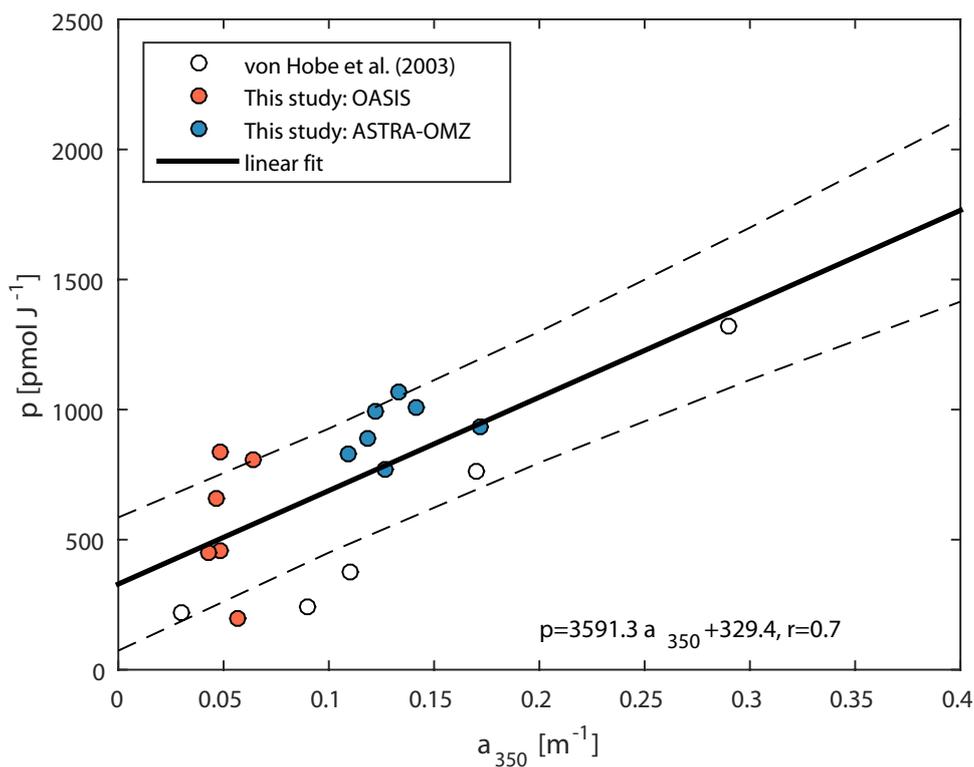
Figure 3. Dependence of photoproduction rate constant p on a_{350} including own fits for p (resulting in blue lines in Fig. 2) and fits from a similar study (von Hobe et al., 2003). Dashed lines indicate the 95% confidence interval.

Table 1. Missing source estimates derived from top-down approaches: The listed studies used an increased vegetation sink and an *a priori* direct and indirect ocean flux to estimate the magnitude of the missing source. Assigning the missing source to oceanic emissions results in the total ocean flux listed here. Fluxes are given in Gg S per year.

Reference	*a priori* ocean flux	missing source	total ocean flux
Suntharalingam et al. (2008)	235	230	465
Berry et al. (2013)	276	600	876
Kuai et al. (2015)	289	800	1089
Glatthor et al. (2015)	276	714	992
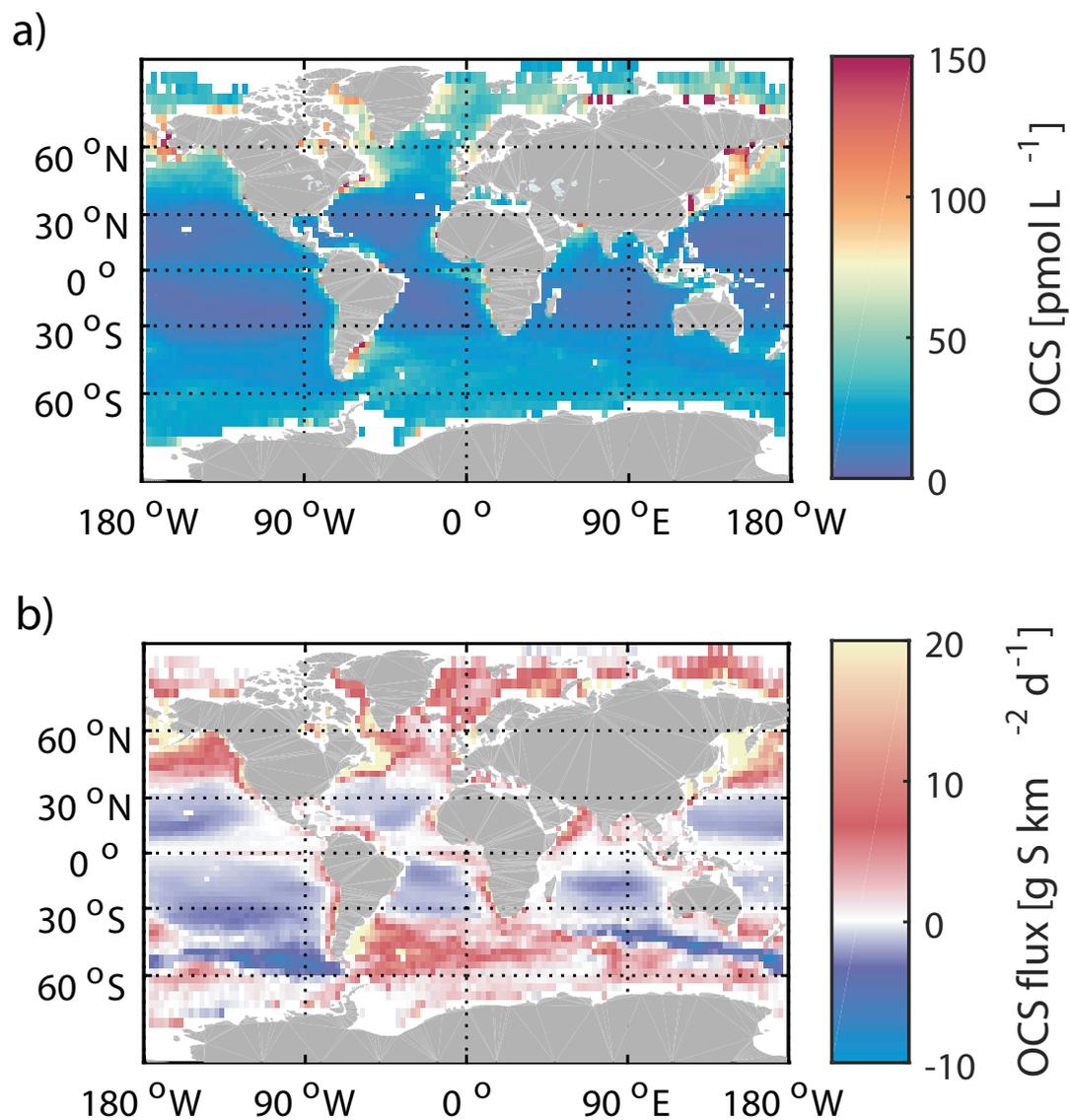
Figure 4. Annual mean of surface ocean concentrations of OCS simulated with the box model (a) and corresponding emissions (b).
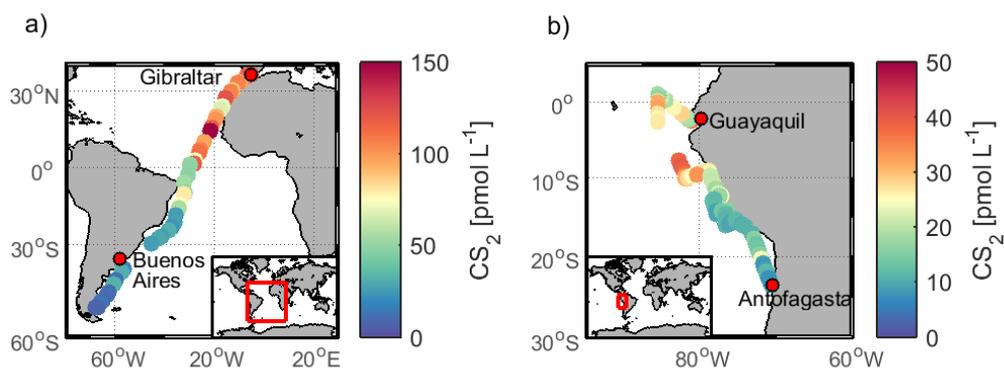
Figure 5. Measured concentration of CS_2 in surface waters during a) ASTRA-OMZ in the East Pacific Ocean and b) TransPEGASO in the Atlantic Ocean.

Table 2. Global oceanic emission estimates of OCS: Direct ocean emission estimates of OCS from bottom-up approaches extrapolated from surface ocean measurements if not stated otherwise. Uncertainties are given in parenthesis as in the original paper either as range or ±standard deviation. ([a] units deviate from original paper, converted to Gg S for comparison, [b] upper limit)

Reference	Emitted S as OCS (Gg S yr^{-1})
Rasmussen et al. (1982)	320 ($\pm$160)[a]
Ferek and Andreae (1983)	245[a]
Johnson and Harrison (1986)	110-210[a]
Mihalopoulos et al. (1992)	230 (110-210)[a]
Chin and Davis (1993)	160 (85-340)[a]
Weiss et al. (1995b)	-16 (10-30)[a]
Ulshöfer and Andreae (1998)	41-80[a]
Watts (2000)	53 ($\pm$80)[a]
Xu et al. (2001)	53[a]
Kettle (2002)	41 ($\pm$154)
Launois et al. (2015a) [model simulation]	813 (573-3997)
This study [box model simulation]	**130**[b]

Table 3. Average, standard deviation and range of parameters observed during the cruises OASIS (Indian Ocean, 2014), ASTRA-OMZ (Pacific Ocean, 2015) and TransPEGASO (Atlantic Ocean, 2014).

		average (± std. dev.)	minimum	maximum
OASIS (Indian Ocean)				
OCS sea surface concentration	[pmol L^{-1}]	9.1 (±3.5)	5.1	20.7
OCS flux	[g S d^{-1} km^{-2}]	-0.25 (±0.5)	-1.6	1.5
SST	[°C]	27.0 (±1.4)	22.2	32.0
salinity	[-]	34.9 (±0.3)	34.3	35.4
wind speed	[m s^{-1}]	7.6 (±2.1)	0.2	14.5
a$_{CDOM}$(350)	[m^{-1}]	0.03(±0.02)	n.d.	0.12
ASTRA-OMZ (Pacific Ocean)				
OCS sea surface concentration	[pmol L^{-1}]	28.3 (±19.7)	6.5	133.8
OCS flux	[g S d^{-1} km^{-2}	1.5 (±2.1)	-1.5	19.9
CS$_2$ sea surface concentration	[pmol L^{-1}]	17.8 (±8.9)	6.7	40.1
CS$_2$ flux	[g S d^{-1} km^{-2}]	4.1 (±3.2)	0.2	14.4
SST	[°C]	20.1 (±2.9)	15.6	26.9
salinity	[-]	35.0 (±0.43)	33.4	35.5
wind speed	[m s^{-1}]	7.4 (± 2.0)	0.3	15.5
a$_{CDOM}$(350)	[m^{-1}]	0.15 (±0.03)	0.1	0.24
TransPEGASO (Atlantic Ocean)				
OCS sea surface concentration	[pmol L^{-1}]	23.6 (±19.3)	2.6	78.3
OCS flux	[g S d^{-1}]	1.3 (±3.5)	-1.7	14.0
CS$_2$ sea surface concentration	[pmol L^{-1}]	62.5 (±42.1)	23.2	154.8
CS$_2$ flux	[g S d^{-1} km^{-2}]	13.7 (±9.8)	0.3	33.9
SST	[°C]	22.6 (±6.3)	7.1	29.6
salinity	[-]	34.9 (±2.6)	28.4	38.1
wind speed	[m s^{-1}]	7.4 (±3.1)	0.4	19.0
a$_{CDOM}$(350)	[m^{-1}]	0.13 (±0.11)	0.0023	0.45